The 14th International Topical Meeting on Nuclear Reactor Thermalhydraulics, NURETH-14
Toronto, Ontario, Canada, September 25-30, 2011

NURETH14-129b

EXPERIMENTAL SETUP FOR THE INVESTIGATION OF FLUID-STRUCTURE INTERACTIONS IN A T-JUNCTION

M. Kuschewski, R. Kulenovic and E. Laurien
University of Stuttgart, Institute for Nuclear Technology and Energy Systems, Stuttgart, Germany
mario.kuschewski@ike.uni-stuttgart.de, rudi.kulenovic@ike.uni-stuttgart.de, eckart.laurien@ike.uni-stuttgart.de

Abstract

The investigation of fluid-structure interactions (FSI) is of mature interest in a number of engineering disciplines. Failures due to fatigue caused by fluid structure interactions are known to the nuclear community. The paper presents first experimental data collected with an experimental setup which brings a new type of induced-fluorescence-system into application. The setup consists of a T-junction of pipes with circular cross-sections with nominal diameter of 80 mm and 40 mm connected to inlet pipes longer than 50 diameters. The optical measurement system utilises the determination of the 2D local water density distribution near the inner wall.

Introduction

Thermal fatigue caused by fluid-structure interactions are known to the nuclear community. Since these problems could be related to the influence of thermal transients and mixing of non-isothermal or stratified coolant flows experimental as well as analytical research were started. Considerable progress was made in dealing with low cycle fatigue (LCF) and today's power plants are equipped with functional monitoring system. Concerning high cycle fatigue (HCF) there is still a lack of reliable experimental data which are required for development of suitable computer models.

On behalf of the BMU (Federal Ministry for the Environment, Nature Conservation and Nuclear Safety) a working group described the methods applied in nuclear power plants to monitor fatigue in piping and vessels [1]. They pointed out that thermal stresses result from temperature transients, temperature imbalances, temperature fluctuations and chiefly from stratifications and streams of temperature. The current temperature monitoring equipment consists of thermocouples which are fixed either through small spot welded clamps or through special clamping devices to allow of removal for inspections. Experience has shown that particularly transients may lead to measuring faults due to delayed response of the sensors and that the maximum detectable fluctuation frequencies are about 1 Hz. Thus, the monitoring systems are suitable for LCF but not for HCF.

Component failures due to HCF are well known from the CIVAUX event. In the residual heat removal system of the French nuclear power plant CIVAUX temperature fluctuation with frequencies higher than 1 Hz lead to damage and cracks in a straight piping, a T-junction and a bend. In publications (e.g. [2]) the HCF mechanism is described as a well known thermo-mechanical phenomenon usually causing elephant skin type damage on surfaces. Before

CIVAUX event, it was commonly admitted that the thermal stripping led to a crack initiation, then an arrest of the crack propagation. Yet the opposite was the case. Further investigations of the thermal loading showed that low frequency temperature fluctuations could be the reason for the rapid through thickness crack propagation. With the aim to understand the coupling of fluid and structure computational fluid dynamics simulations were carried out for the thermo-hydraulics and thermo-elastic calculations of stresses in thermo-mechanics. The damage is explained by important temperature differences between cold and hot water flows [2] at specific wall locations with fluctuation frequencies between 2 to 10 Hz.

1. Vattenfall Experiment

Besides others the OECD/NEA Vattenfall experiment [3] has become generally known as a benchmark experiment for the validation of CFD-models. It is a sharp edge 90° T-junction experiment made of transparent polymer (Fig. 1). A vertically aligned side branch of 100 mm ID is attached perpendicular to a larger pipe with 140 mm ID. The fluid used was water and a temperature difference about 17 K was set for the experiments.

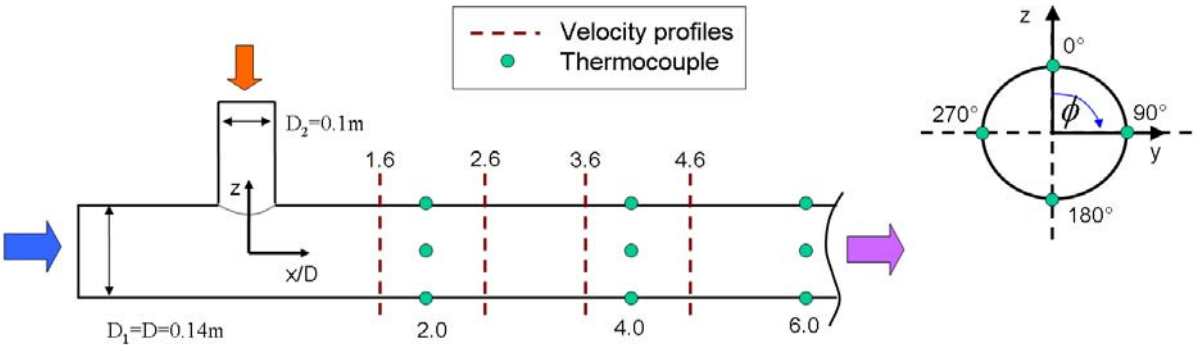

Figure 1 OECD/NEA Vattenfall benchmark experiment

The velocity profiles and the corresponding RMS values were determined for the inlets. For the mixing zone the velocity profiles and temperature information were collected at specific positions x/D. The experimental data were especially used for the validation of large eddy simulations (LES) which showed promising results. The used models applied adiabatic wall conditions and do not recognise dominance of buoyancy effects which become dominant for high temperature differences. The temperature increase was restricted by the material characteristics of the polymer and the maximum refractive index difference in the fluid domain given by the optical measurement principles.

2. New Fluid-Structure Interaction Setup

For a better understanding of the fluid-structure interaction (FSI) under consideration of heat transfer from the fluid to the wall and from the wall to the fluid a new experimental setup is built up within a joint research project. The setup (see Fig. 2) comprises a closed water loop with a three stage membrane booster pump and a circulation pump.

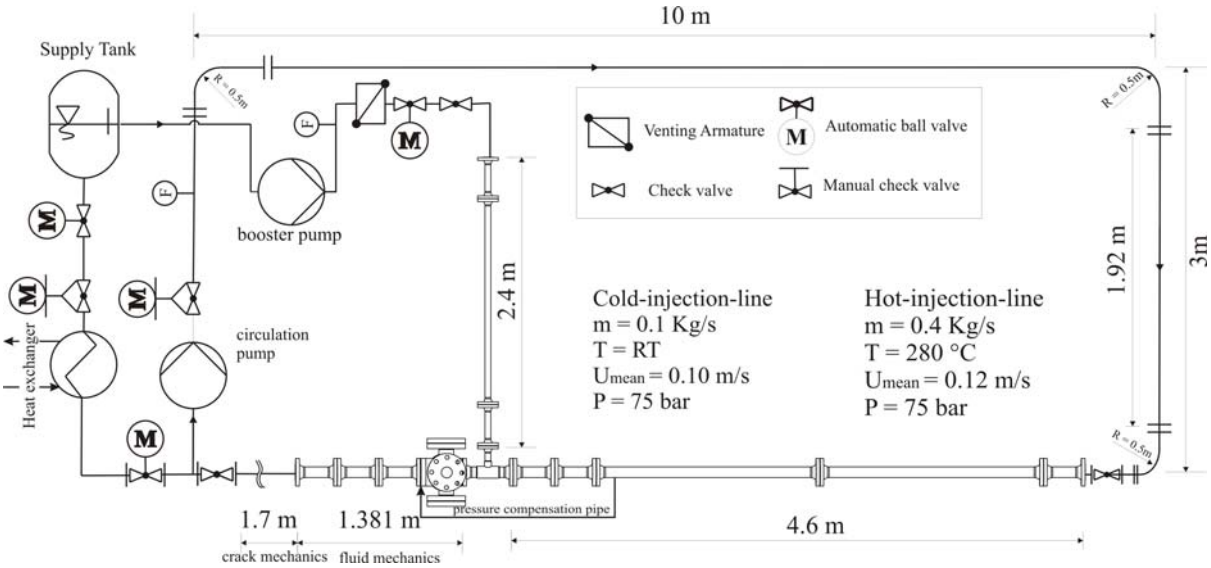

Figure 2 Simplified piping and instrumentation diagram

The cold injection (ID 38.9 mm) line is fed directly with the pressurised water (ambient temperature, 75 bar) from the supply tank. The water for the hot injection line (ID 71.8 mm) is heated up via resistance heating. The maximum water temperature is 280 °C. Both injection lines have with lengths of more than 50 diameters and include rectifiers. The water flows are combined in a horizontally aligned sharp edge 90° T-junction and mix in the outlet line (ID 71.8 mm) with a length of 3.4 m. The T-junction is surrounded by different interchangeable modules connected by means of flanges. For each pipe diameter an optical module is available (see Fig. 3). They comprise glass pipes surrounded by a pressure vessel filled with water. Flanges with glass windows enable an optical access to the glass pipes from outside and the application of optical measurement techniques.

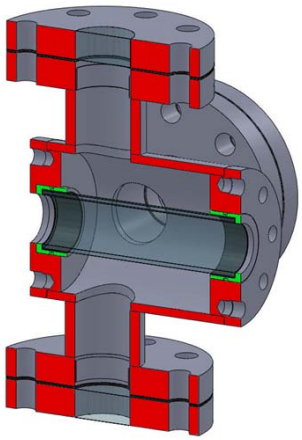

Figure 3 Optical module

3. Experimental setup for the investigation of FSI

3.1 Inlet conditions

For the validation of computational fluid dynamics models it is essential to collect information regarding the boundary conditions. The mass flow rate for the main and branch line and the corresponding mean temperatures are measured conventionally (flowmeter, thermocouple). Velocity distributions are also needed and determined with the well-known Particle-Image-Velocimetry (PIV).
For the classical two-components PIV (2C-PIV) an optical access with two perpendicular windows is needed. A sheet of laser light is orientated trough one window parallel to the pipe axis. A specialised camera is installed perpendicular to the light sheet and zooms on seeding particles in the flow illuminated within the light sheet. Comparing a time-series of pictures makes it possible to detect the movement of groups of particles in the time intervals between the pictures. The time differences are known, thus the velocity of particle groups can be expressed in pixels per second. By means of a length calibration it is possible to map pixel values to real dimensions and ultimately calculate local velocity distributions i. e. the two velocity components within the measurement plane.

3.2 Optical conditions of the mixing zone

The application of non-invasive optical measurement techniques for flows with a change of the refractive index is always challenging and often not possible. In Fig. 4 (left) a refractive index

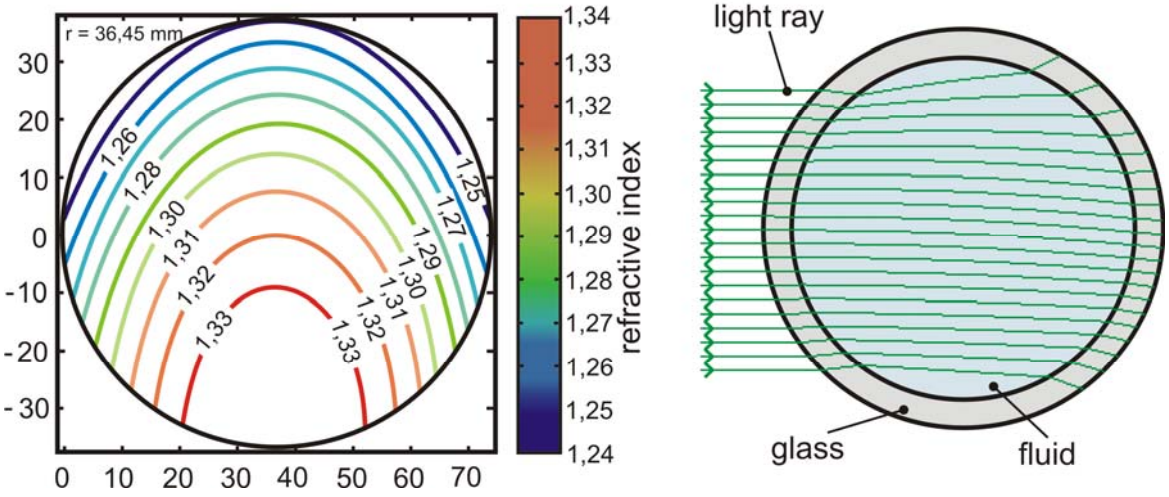

Figure 4 Example snapshot for a refractive index distribution (left) and the corresponding light ray calculation performed with Zemax (right)

distribution is shown. It corresponds qualitatively to temperature distributions in a mixing pipe known from T-junction experiments (see [4]). For the illustration the values were scaled for the case of combining flows of non-isothermal water with 25 °C resp. 280 °C and 75 bar.
The corresponding values of the refractive index for green light range from 1.336 for cold water to 1.249 for hot water with an increasing gradient in direction of smaller values.

The ray tracing calculation is performed with Zemax. The values for the fluid are imported and the model completed with a glass tube (two shells) and a water buffer around it. A collimated monochromatic light source with 532 nm is used and a selection of 21 rays is shown in Fig. 4 (right). One can see the refraction effect when the rays enter and leave the glass. In the mixing fluid domain the light refraction is a distribution in space. This leads to curved rays. The effect gets stronger for regions where the gradient of the refractive index is perpendicular to the ray propagation direction.
The introduced refractive index distribution came out of an averaged temperature distribution. Taking into account a realistic, strongly disturbed and unsteady flow regime it is obvious that any optical measurement technique which depends on a static ray distribution in the fluid is not feasible. Therefore, a new measurement technique is applied for this problem.

3.3 Novel Near-Wall-LED-Induced-Fluorescence technique

For some experimental investigations of thermo-hydraulic problems with liquids it is gainful to apply temperature sensitive dye which is homogenously mixed with the liquid. At the position of interest an optical access is needed. Usually a laser light sheet is used to stimulate the dye particles in a thin layer to emit fluorescence light which can be recorded with a camera system. Herby most of the light passes the measurement region without being absorbed. The fluorescence light emission of the dye strongly depends on the excitation intensity and the dye temperature. With a known excitation it is possible to measure the temperature distribution in the observe layer. As described above the optical conditions make it impossible to associate the local light emission with a temperature. Therefore, a modified thermometry technique is introduced on the basis of a light emitting diode (LED).
The diode is aligned with the optical axis of the camera and illuminates the pipe from one side. The dye concentration in the fluid is selected so high that the whole light is absorbed. The length in which 95 percent of the light is absorbed is defined as penetration length. With penetrations lengths of about 1 mm the refraction effect in the mixing zone can be neglected because the path lengths of the rays are short. The camera detects the light coming from the illuminated thin dye layer which is now associated to a specific local temperature distribution.
If the fluid flow system has no temperature differences the described technique must be changed slightly. Instead of mixing one dye homogenously in the liquid two different dyes are used. For the case of the T-junction experiment each inlet line is marked with another dye. It does not matter if one dye has fluorescent properties or both. The two dyes are mixed i.g. in a T-junction and the detected fluorescence intensity near the wall is then proportional to the mixing scalar (dye fraction). For the mapping of the mixing scalar to temperature values a calibration is needed. For this purpose two cuvettes are filled with water from each supply tank of the T-junction lines. A third cuvette is filled with a half-and-half mixture. The cuvettes are placed in the optical path of the measurement setup and reference pictures are recorded. The recognised fluorescence intensity difference is used to complete the transformation equations:

$$\rho_{mixture} = f_1\left(\frac{I_{dye1}}{I_{dye2}}\right); \qquad \mathrm{T} = f_2(\rho_{mixture}) \tag{1}$$

Detailed information regarding the Near-Wall-LED-IF technique can be found in [5].

3.4 Cold setup for the demonstration of the measurement technique

The application of the near wall LED-IF was tested with a second T-junction setup. The so called PVC-testrig is partly made of transparent and in-transparent PVC-pipes and joints. A simplified schematic of the piping and instrumentation diagram is shown in Fig. 5.

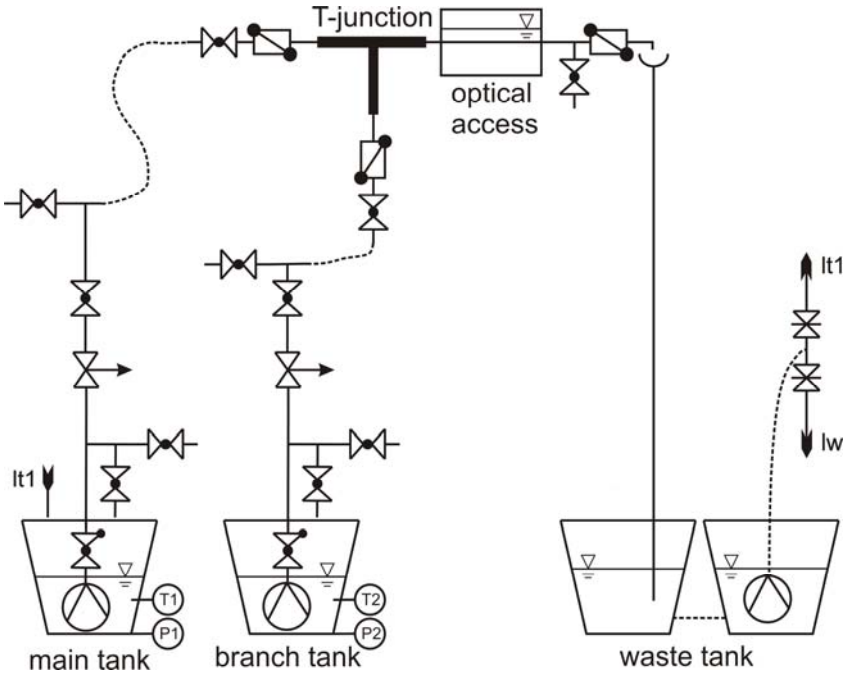

Figure 5 Simplified schematic of the PVC-testrig

Like for the FSI setup the 90° T-junction is horizontally aligned. Yet the PVC-testrig comprises an open loop with two separated supply tanks and a waste water tank. For each tank an immersion pump is used to either control the mass flux for the inlets or empty the waste tank. Ball valves and inclined seat valves are installed for the fine adjustment. The inner diameters of the pipes (ID branch line 35.5 mm and ID main line 71 mm) were selected to minimise the difference to the FSI-setup. For the optical access also a glass tube is used. It is surrounded by an aquarium made of transparent PVC and glass elements. It is filled with water to compensate the refractive index difference of water, glass and air. Downstream of the aquarium two pipe elements are installed before a hose feeds the water in the waste tank. Each one has a length of 340 mm (4.7 diameters) so that a feedback of the out flowing fluid can be neglected.
The volume flux is calculated with the help of hydrostatic pressure transducers. For this purpose the increased density must be taken into account. It is measured separately with a beaker and a balance before the test.

4. Experimental Results

The near wall LED-IF technique was applied at the cold PVC-testrig. In Tab. 1 the chosen settings for the test experiment are shown. The supply tank for the branch line was seeded with sugar (saccharose) to increase the density. For this purpose 43,62 kg sugar was soluted in

222,5 liter tap water. The resulting density difference between the two inlet lines is close to a density difference for a non-isothermal mixing of water with 25 °C and 131 °C (75 bar). All data presented were calculated with the formulations of the National Institute of Standards and Technology and additionally documented equations found in [6] to [9].

$$\frac{\rho_{water\,25°C,75bar}}{\rho_{water\,131°C,75bar}} = \frac{1000}{937.8} \approx 1.0663 \approx \frac{\rho_{sugarwater\,(brix=16.38)}}{\rho_{water\,20°C,std.pressure}} = \frac{1065}{998.2} \approx 1.0669$$

The sugar also changes the speed of light in the water and the resulting refractive index fraction is close to the condition of non-isothermal mixing of water:

$$\frac{n_{sugarwater\,(brix=16.38)}}{n_{water\,20°C,std.pressure}} = \frac{1.358}{1.335} \approx 1.0172 \approx \frac{n_{water\,25°C,75bar}}{n_{water\,131°C,75bar}} = \frac{1.336}{1.313} \approx 1.0175$$

The main difference can be found in the viscosity ratios due to the strong reduction in viscosity for increased water temperatures:

$$\frac{\eta_{sugarwater\,(brix=16,38)}}{\eta_{water\,20°C,std.pressure}} = \frac{1.664}{1.0016} \approx 1.661 < \frac{\eta_{water\,25°C,75bar}}{\eta_{water\,131°C,75bar}} = \frac{0.8885}{0.213} \approx 4.17$$

Latter is the reason why the *Re*-similarity cannot be fulfilled for this cold setup. However it is not the intention of this study to reproduce exactly the flow conditions of the hot setup in the cold testrig. The first application of the near-wall measurement technique is the main focus here. In comparison the density difference is 13 times higher than for the Vattenfall experiment. While the resulting refractive index difference due to the sugar is increased up to 1.72 percent which is 10 times higher than for the Vattenfall case and much higher than any published experiment known to the authors.

Table 1 System settings and fluid parameter for the test experiment

branch line (ID 35.5 *mm*)	20 *°C*, 1500 *l/h*, *Re* = 9576, $\rho_{sugarwater\,(brix=16.38)} = 1065\ kg/m^3$
main line (ID 71 *mm*)	20 *°C*, 3000 *l/h*, *Re* = 14894, $\rho_{water\,20°C,std.pressure} = 998.2\ kg/m^3$
combined line	20 *°C*, 4524 *l/h*, *Re* = 20066, $\rho_{water\,20°C,mixture} = 1015\ kg/m^3$
associated temperature difference	106 *K*
density difference	$\frac{\rho_{sugarwater\,(brix=16.38)} - \rho_{water\,20°C,std.pressure}}{\rho_{water\,20°C,std.pressure}} = 6.69\ \%$
refractive index difference	$\frac{n_{sugarwater\,(brix=16.38)} - n_{water\,20°C,std.pressure}}{n_{water\,20°C,std.pressure}} = 1.72\ \%$
measurement position	*x/D* = 5
penetration depth	1 *mm*
observation region	36 x 47 *mm²*

With the Near-Wall-LED-Induced-Fluorescence technique the local dye-fraction is measured. It is assumed that for the describe configuration it is proportional to the local density which itself is transformed into a temperature. For comparison reason the same nomenclature as for the Vattenfall analyses are used.

$$T^*_{mean} = \frac{\overline{T - T_{cold}}}{T_{hot} - T_{cold}}; \quad T_{RMS} = \sqrt{\overline{((T - T_{mean})^2)}}; \quad T^*_{RMS} = \frac{T_{RMS}}{\Delta T} = \frac{T_{RMS}}{T_{hot} - T_{cold}} \tag{2}$$

The associated local temperature calculated from the local density (dye fraction) is denoted as T while T_{hot} and T_{cold} are the associated temperatures of the inlets.

The LED camera system was aligned parallel to the branch line 5 diameters downstream of the T-junction. The dimensions of the observation region were 36×47 mm^2. The concentration of the dyes and the LED power was chosen such that the penetration depth was 1 mm. Before the test run the pipes were filled with water from both tanks.

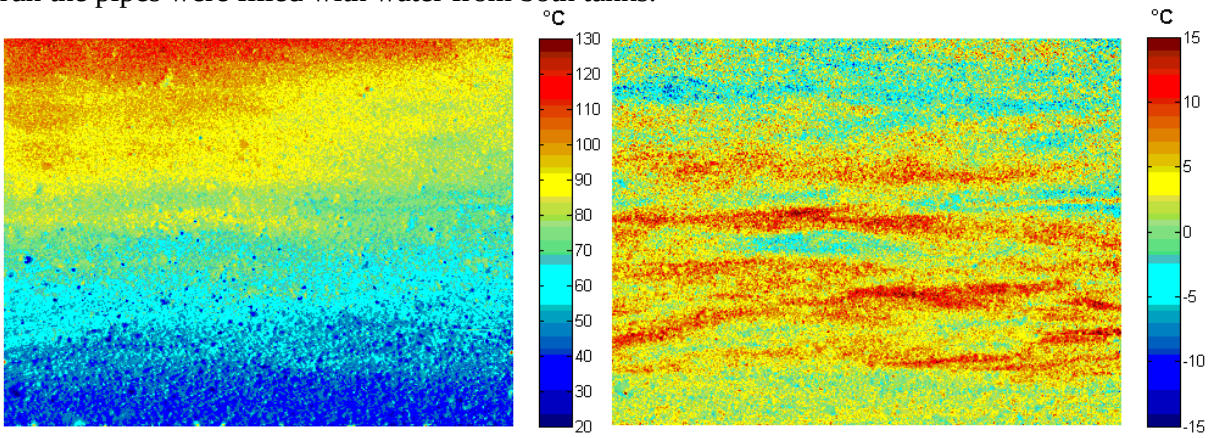

Figure 6 Temperature fields calculated from measured fluorescence light distributions at downstream position x/D = 5 (left: snapshot, right: deviation from local mean temperature)

In the time between back filling of the pipes, venting and start of the test run the fluid settled and layered. The first picture was taken 50 *s* after starting the pumps. For this run a number of 400 pictures were recorded in 50 *s*. The pictures are corrected for the LED light distribution and scaled using the cuvette calibration data. In Fig. 6 (left) a snapshot of the calculated temperature field is shown.

It can be clearly seen that the fluid flows are not perfectly mixed. The less dense fluid (associated hot fluid) is flowing over the sugar seeded fluid (associated cold fluid) from the branch line. The time series shows fluctuating temperatures in the whole measurement field. Averaging over time and subtracting the result from the snapshots gives the temperature fluctuation resp. the deviation from the mean temperature field. The deviation range is ±15 *K* (Fig. 6 right). This corresponds to ±13.6% of the inlet temperature difference.

For the local analysis the pictures are divided into 16x16 pixel segments. This equals a square with physical dimensions of approximately 0.56 mm x 0.56 mm. For every time step the mean temperatures of the segments are calculated. The resulting temperature variation time-series with respect to the local mean temperature for the segment in the middle of the region of observation is shown in Fig. 7 left. The associated temperatures vary in the range of +12.5 °*C* to -16.4 °*C* for the observed time interval of 50 s which corresponds to *T** values between 0.54 and 0.27. On the basis of the time-series for every segment the mean *T**-value and its corresponding rms-value T^*_{RMS} are calculated. For the selection of 5 axial positions on the centreline the normalised temperatures are shown in Fig. 7 right.

The normalised mean temperature is decreasing for increasing axial distances. The rms-values decrease too but not proportional to it. According to the inlet conditions the normalized

temperature T^* for a perfect mixture is 0.75. Due to the reason that the observed T^*-values are below this value and are further decreasing one can state that the final mixture is not yet achieved at the position x/D=5. The reason for the reduction of the associated normalised temperatures can be explained when buoyancy effects are taken into account. In other mixing experiments of fluids with different densities (e. g. [4]) a buoyancy driven swashing motion of the fluids was identified. The more dense sugar water from the side branch is pulled down to the bottom of the pipe while the water without sugar added is displaced. This stratification is not stable so that the interface between these two fluid streams is twisted. The behaviour of this interface, the linked influence parameter and the impact on the fluid structure interactions will be subjects of future investigations.

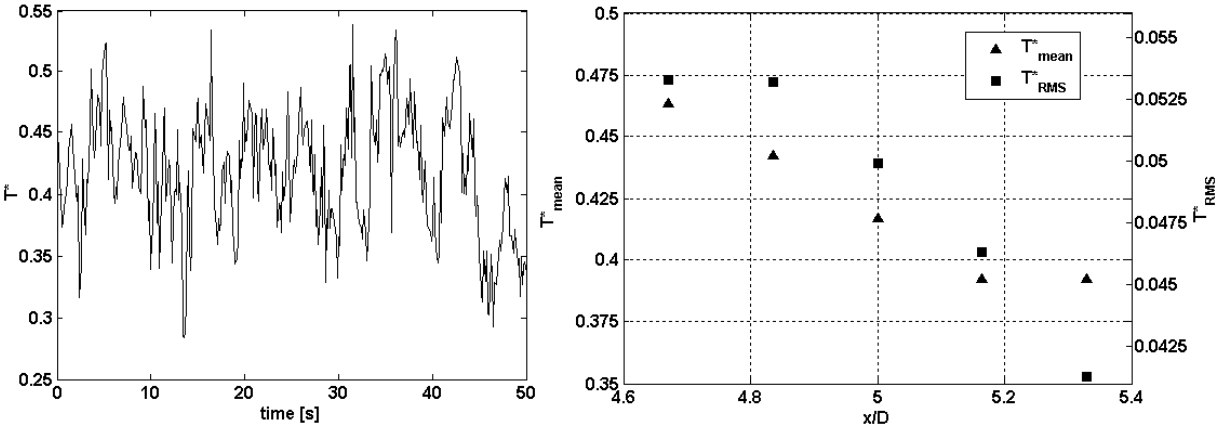

Figure 7 Temperature variations calculated for a monitored area in the centre of the measurement area (left), normalised temperatures and rms-values for different axial positions (right)

5. Summary

A new experimental T-junction setup for the investigation of fluid-structure interactions has been introduced. It provides a maximum water temperature of 280 °C and a system pressure of 75 bar. For the investigation of the mixing zone a novel application of an induced fluorescence technique (Near-Wall-LED-Induced-Fluorescence) was applied for a second, geometrically similar cold T-junction setup, and two water flows with a density difference of 6.69 % were mixed in a horizontal oriented T-junction. Sugar was used to increase the density (simulation of temperature induced density variations) and two dyes were used to mark the water of the branch and the main line. The resulting refractive index difference due to the sugar was increased up to 1.72 percent which is 10 times higher than for the Vattenfall case and much higher than any published experiment with optical flow applications known to the authors. Five diameters downstream of the intersection the local dye fractions were detected with a camera setup and the local densities and the associated temperatures were calculated. It was shown that unsteady temperature fields in a liquid flow near the wall ca be observed even under flow conditions with refractive index differences of about 1.7%. The experimental results prove that the flow is not perfectly mixed and indicate the existence of a twisted interphase between the two water flows.

6. Acknowledgement

This work is carried out in the frame of a current research project funded by the German Federal Ministry of Education and Research, project number 02NUK009B.

7. References

[1] P. Hofstötter, S. Dittmar, K. Maile, K. J. Metzner, ”In-Service monitoring of piping and vessels in nuclear power plants: report on BMU Study SR 2218”, *Nuclear Engineering and Design*, Vol. 193, 1999, pp. 233-241.

[2] S. Chapuliot, ”Thermal fatigue in mixing areas”, Keynote lecture of the Kick-Off meeting for the OECD/NEA CFD Benchmark Task, Areva, OECD/NEA, Issy-les-Moulineaux, France, 2009 May 20.

[3] K. Angele, ”The Vattenfall T-junction test facility”, Lecture of the Kick-Off meeting for the OECD/NEA CFD Benchmark Task, Vattenfall, OECD/NEA, Issy-les-Moulineaux, France, 2009 May 19.

[4] H.-M. Prasser, A. Manera, B. Niceno, M. Simiano, B. Smith, C. Walker, R. Zboray, ”Fluid Mixing at a T-junction”, Proceedings of the Workshop on Experiments and CFD Code Application to Nuclear Reactor Safety, Grenoble, France, 2008 Sept.10-12.

[5] M. Kuschewski, R. Kulenovic, E. Laurien, ”Novel Application of LED-Induced Fluorescence”, Proceedings of the Anual Meeting of the German Association for Laser Anemometry, Ilmenau, Germany, 2011 Sept. 6-8.

[6] H. Schiweck, P. W. van der Poel, T. Schwartz, “, Zuckertechnologie: Rüben- und Rohrzuckergewinnung“, Bartens, Germany, 2000.

[7] Release on the IAPWS Formulation 1995 for the Thermodynamic Properties of Ordinary Water Substance for General and Scientific Use, 1996.

[8] W. Wagner and A. Pruß, “The IAPWS Formulation 1995 for the Thermodynamic Properties of Ordinary Water Substance for General and Scientific Use,” *J. Phys. Chem. Ref. Data*, 31, 387, 2002.

[9] A.H. Harvey, J.S. Gallagher, and J.M.H. Levelt Sengers, "Revised Formulation for the Refractive Index of Water and Steam as a Function of Wavelength, Temperature and Density," *J. Phys. Chem. Ref. Data*, 27, 761, 1998.